

Afferent Input Regulates the Formation of Distal Dendritic Branches

ADI MIZRAHI* AND FREDERIC LIBERSAT

Zlotowski Center for Neuroscience and Department of Life Sciences, Ben-Gurion University of the Negev, 84105 Beer-Sheva, Israel

ABSTRACT

During postembryonic development, the dendritic arbors of neurons grow to accommodate new incoming synaptic inputs. Our goal was to examine which features of dendritic architecture of postsynaptic interneurons are regulated by these synaptic inputs. To address this question, we took advantage of the cockroach cercal system where the morphology of the sensory giant interneurons (GIs) is uniquely identified and, therefore, amenable to quantitative analysis. We analyzed the three-dimensional architecture of chronically deafferented vs. normally developed dendritic trees of a specific identified GI, namely GI2. GI2 shows five prominent dendrites, four of which were significantly altered after deafferentation. Deafferentation induced an average of 55% decrease in metric measures (number of branch points, total length, and total surface area) on the entire dendritic tree. Sholl and branch order analysis showed a decrease in the most distal and higher order branches. We suggest that afferent input plays a specific role in shaping the morphology of dendritic trees by regulating the formation or maintenance of high-order distal branches. *J. Comp. Neurol.* 452: 1–10, 2002. © 2002 Wiley-Liss, Inc.

Indexing terms: 3D reconstruction; deafferentation; morphometry

Dendritic architecture plays a crucial role in determining connectivity patterns within neural networks. In addition, the architecture of dendritic trees modulates the basic biophysical properties (Rall et al., 1992; Koch and Segev, 2000) and the firing patterns (Mainen and Sejnowski, 1996; Vetter et al., 2001) of neurons. In vivo imaging shows that development of dendritic trees is a highly dynamic process of membrane expansion and retraction (Cline, 1999, 2001). A major issue in neuronal development is to determine how the maturation of dendritic trees is regulated by both intrinsic and extrinsic signals. Several molecular and cellular elements, such as intracellular proteins, extracellular trophic factors, and synaptic activity, have been suggested to play a role in dendritic morphogenesis (Acebes and Ferrus, 2000; Cline, 2001; Scott and Luo, 2001). Afferent innervation from presynaptic neurons to dendrites has direct consequences for the establishment of the mature morphology of dendritic trees as well (Gray et al., 1982; Smith et al., 1983; Deitch and Rubel, 1984). The goal of this work was to characterize quantitatively the morphologic effects of sensory deprivation on the dendritic arborizations of central neurons. Specifically, we aimed to determine which features of mature dendritic architecture are altered after long-term deafferentation. We analyzed the three-dimensional (3D) architecture of chronically deafferented

vs. normally developed dendritic trees of a specific identified giant interneuron (GI) in the cercal system of the cockroach.

The cercal system serves as a good model for deafferentation studies because it has been characterized from early embryonic stages through adulthood (Daley et al., 1981; Blagburn and Beadle, 1982, 1984; Daley and Camhi, 1988; Blagburn and Thompson, 1990; Hamon et al., 1994; Blagburn et al., 1996). The cercal system consists of a relatively small number of pre- and postsynaptic neurons, which can be identified unequivocally (Daley et al., 1981; Camhi, 1984; Hamon et al., 1994). Wind receptors located on posterior sense organs called cerci provide the major

Grant sponsor: Israel Academy of Sciences and Humanities; Grant number: 335/00-1.

Dr. Mizrahi's current address is Department of Neurobiology, Duke University Medical Center, P.O. Box 3209, Durham, NC 27710.

*Correspondence to: Adi Mizrahi, Department of Neurobiology, Duke University Medical Center, P.O. Box 3209, Durham, NC 27710. E-mail: mizrahi@neuro.duke.edu

Received 26 September 2001; Revised 29 January 2002; Accepted 2 April 2002

DOI 10.1002/cne.10275

Published online the week of August 19, 2002 in Wiley InterScience (www.interscience.wiley.com).

sensory input to three pairs of bilateral GIs in the sixth, or last, abdominal ganglion (Camhi, 1984). The sensory neurons of each cercus project to the last abdominal ganglion and terminate in the ipsilateral portion of the neuropile. There they establish contact with the major dendritic arborizations ipsilateral to the axon of the GI (Fig. 1A). Each GI sends its large axon through the nerve cord and reaches the locomotory centers in the three thoracic ganglia where it excites specific thoracic interneurons, which in turn excite leg motor neurons (Ritzmann, 1984). When the GIs are already differentiated at late embryonic stages, only two sensory neurons are present on each cercus of the first instar larval stage (Bugnion, 1921; Dagan and Volman, 1982). During postembryonic development, after each consecutive molt, new filiform hairs are added to the cerci. Thus, on each cercus, the number of sensory neurons increases from two hairs in the first instar to 220 in the adult cockroach. In parallel, the dendritic trees of the GIs grow in size to accommodate the new incoming synaptic inputs. One mechanism by which the GIs grow to accommodate additional inputs involves synaptic re-organization (Chiba et al., 1988). In that respect, the architecture of the GIs matures in such a way as to preserve their electrotonic properties (Hill et al., 1994).

Given that the GIs develop in conjunction with increasing numbers of sensory neurons and because the morphology of their dendrites is inherently identified, we addressed the following question: Which specific structural features of the dendritic tree are controlled by the input from sensory afferents? Our approach was to amputate a single cercus throughout postembryonic development and analyze quantitatively the dendritic morphology of a specific GI in the adult. Because the normal connectivity pattern of the cercal-to-GI system is dominated by ipsilateral synapses (Daley and Camhi, 1988; Hamon et al., 1994), deafferentation will dramatically affect the synaptic input to the ipsilateral dendritic tree. In the cricket cercal system, this deafferentation of the GIs result in 40% reduction in the length of the main dendritic tree of the deafferented GI (Murphey et al., 1975). Given the recent advances in staining, 3D reconstruction, and morphologic analysis (Mizrahi et al., 2000) we carried out deafferentation of the cockroach cercal system to obtain detailed information and evaluate quantitatively the morphologic effects of deafferentation on dendritic geometry.

MATERIAL AND METHODS

Animals

Male and female cockroaches (*Periplaneta americana*) from the laboratory colony were used for this experiment. Egg cases were collected from female cockroaches, maintained in humid vials, and inspected daily until hatching. Hatchlings were collected, cool anaesthetized, and a single cercus was amputated under the microscope with sharp forceps. Herein after, cockroaches were raised in small plastic cages, kept at 27–32°C, and provided with water and cat chow, ad libitum. Because cockroaches develop a new cercal stump after each molt, they were inspected weekly for molting. Upon molting, animals were cool anaesthetized and the newly developed cercal stump was amputated. Thus, animals were chronically deprived of a single cercus throughout their entire postembryonic life. Animals that reached adulthood were used for staining an individual GI.

Staining, reconstruction, and alignment

The GI staining, 3D reconstructions, and alignment are described in detail in Mizrahi et al. (2000). Briefly, freshly molted adults (within the first week after the molt) were cool anesthetized (2°C) and pinned dorsal side up on a wax platform, and the ventral nerve cord was exposed. GI2 was impaled either in the axon (between the A5–A6 connectives) or in the soma with a glass microelectrode (tip resistance 20–40 M Ω) and filled with 2% Neurobiotin in 1 M KCl for 30–60 minutes, followed by a diffusion period of 1 hour. The abdominal nerve cord was fixed in 2.5% glutaraldehyde in Millonig's buffer (MB), pH 7.4, dehydrated, transferred to propyleneoxide and then rehydrated into MB. The ganglion was then incubated in collagenase/Dispase (1 mg/ml) in MB at 37°C for 1 hour and incubated overnight in avidin-conjugated horseradish-peroxidase (Vectastain Elite ABC-kit) diluted in tritonated MB. Subsequently, the tissue was processed with diaminobenzidine and mounted in Permount medium. Each neuron was visualized through a BH-2 Olympus microscope with an immersion oil lens (100 \times ; NA-0.8; working distance, 0.66 mm). Neurons were reconstructed in 3D by using NeuroLucida (MicroBrightfield, Ltd). Only neurons filled to the tip of the finest distal dendrites were reconstructed. We also reconstructed the fiducials of the ganglion, which house the GIs for GI alignment as described below. Control GI2s ($n = 10$) are neurons from our morphologic database (Mizrahi et al., 2000).

Alignment and scaling

The alignment of the GIs was done in two steps using the NeuroLucida software. First, all the GIs were rotated based on a method described by Jacobs and Nevin (1991). Briefly, the fiducials of each ganglion containing a stained neuron were reconstructed at low magnification (20 \times). Because the ganglion has an elliptic shape, we were able to calculate the three axes from these fiducials (left/right, X axis; anterior/posterior, Y axis; ventral/dorsal, Z axis). Each reconstruction was rotated independently based on these three axes into a straight (parallel) axial set.

Second, each GI shows a common morphologic feature, which is the junction between the link segment, the axon, and the main dendritic tree. We refer to this feature as the alignment node (AN). All GIs were aligned at their AN (Mizrahi et al., 2000).

Morphometric analysis

GIs were examined quantitatively by measuring morphometric parameters such as number of branch points, total dendritic length, and total dendritic surface area. Segment analysis was used to assess branch order distribution. All the above parameters were calculated by using Neuroexplorer (MicroBrightfield, Inc.).

We combined Sholl and branch order analysis to examine the changes in the branching pattern of GI2 as a result of deafferentation. The Sholl analysis measures the occurrence of a given metric parameter between two consecutive spherical shells (Sholl, 1953). All neurons were aligned to the node between the axon and the dendritic tree and concentric spheres, spaced 20 microns apart, were centered at this alignment node. The number of branch points within each sphere was measured in deafferented and control dendritic trees. To evaluate whether spatial or topologic parameters were affected by the ab-

sence of afferent input, we also constructed dendrograms and calculated the frequency distribution of the number of dendritic branches as a function of branch order in deafferented and control dendritic trees. To evaluate changes in tree topology, we used the measure of tree asymmetry (van Pelt et al., 1992). Tree asymmetry is the mean value of partition asymmetries in the tree. The asymmetry value equals zero when at each bifurcation the two subtrees in the pair have an equal number of terminal segments (maximal symmetry). It approaches value one when one of the two subtrees consists of one terminal segment (maximal asymmetry).

Statistical analysis

For the analysis of morphologic differences we used a Student *t* test or analysis of variance (ANOVA). Significance was accepted at *P* < 0.05.

The photomicrographs shown in Figure 2A were taken through a compound light microscope (Olympus BH2) equipped with integrated computerized control of digital camera using a 10× objective. Optical sections were acquired at 5-μm steps and were collapsed as a projection image, and compensated for brightness and contrast by using IPLab Spectrum software.

RESULTS

Postembryonic development of *Periplaneta americana* (from hatching to adult) lasts 10–12 months. We collected female and male hatchlings and chronically amputated a single cercus throughout postembryonic development. We then compared the dendritic morphology of deafferented vs. control GI2s in freshly molted adult animals.

A projection image of a 3D reconstructed GI2 from a freshly molted control adult cockroach is shown in Figure 1B. Morphologically, GI2 can be identified based on its characteristic dendritic geometry and the position of the soma within the neuropile (see also Daley et al., 1981). Furthermore, GI2 has five major identified dendritic trees (Fig. 1C). These five dendrites radiate from the dendritic root in different XY and Z planes. Thus, based on 3D information, the five dendritic trees were identified in all 10 control GI2s from the database. We analyzed the dendritic trees both as whole trees and as individual dendrites.

Deafferentation decreases dendritic tree size

Deafferented dendritic trees appear considerably smaller than the controls. The effect of deafferentation is illustrated in Figure 2A with a representative example of double staining of a pair of GI2s from a control and a deafferented animal. Three reconstructed examples of control and deafferented GI2s are shown in Figure 2B and 2C, respectively. Quantitative morphometric analysis reveals that the number of branch points, total length, and total surface area significantly decreases (*t* test, *P* < 0.01 for all parameters) by 42%, 50%, and 51%, respectively (Fig. 3A). Although there is a prominent decrease in dendritic size, the main architectural features are conserved and all cells are readily identified as GI2.

To study whether deafferentation equally affected all five identified dendrites of GI2, we also carried out a morphometric analysis for each individual dendritic tree. Analysis of the number of branch points, total length, and total surface

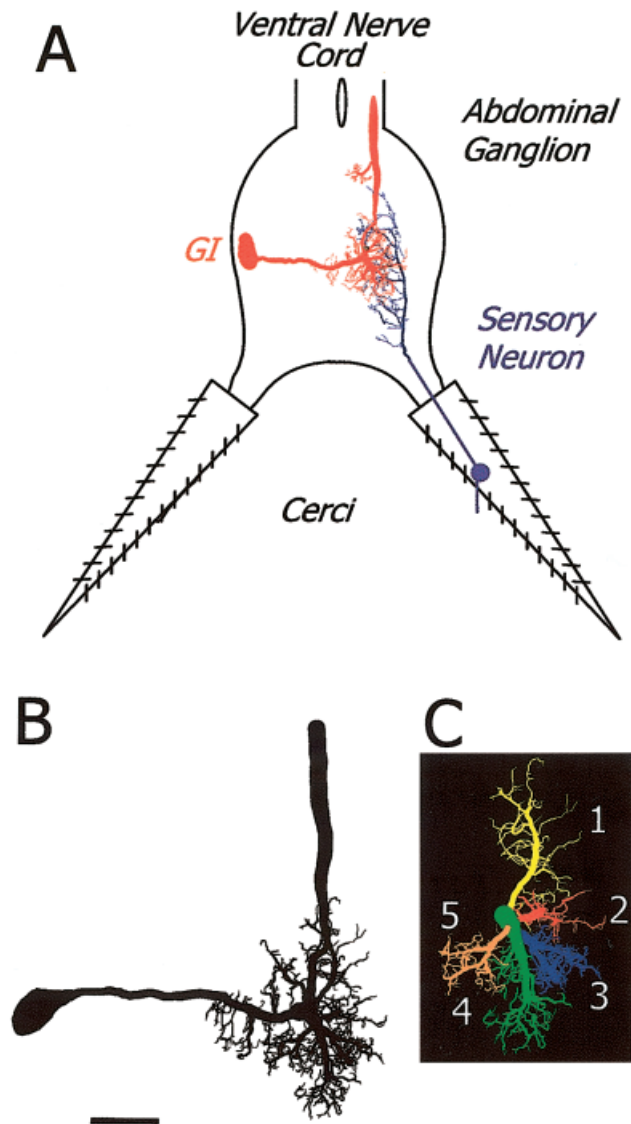


Fig. 1. Identified dendritic trees of the cercal system of the cockroach. **A:** Schematic drawing of the last abdominal ganglion and the two cerci. Sensory neurons (an example is shown in blue) project their axons into the neuropile of the last abdominal ganglion. There, they mainly innervate the dendritic trees of the giant interneurons (GIs) on the ipsilateral side of the ganglion (one GI is shown in red). **B:** Three-dimensional reconstruction of GI2 from a control animal in a dorsal view. **C:** Five identified dendrites shown in different colors and numbered clockwise can be identified in the reconstructed GI2 shown in B. Scale bar = 100 microns in B.

area revealed that dendrites number 2 and 4 were most affected by deafferentation and dendrites number 1 and 5 were affected by deafferentation but to a lesser extent (Fig. 3B). By contrast, dendrite number 3 seems to be unaffected by chronic deafferentation as all three metric parameters were not significantly changed (Fig. 3B).

Sensory input promotes the formation or maintenance of distal branches

Subsequently, we wished to explore which specific morphologic features of the dendritic tree were affected by

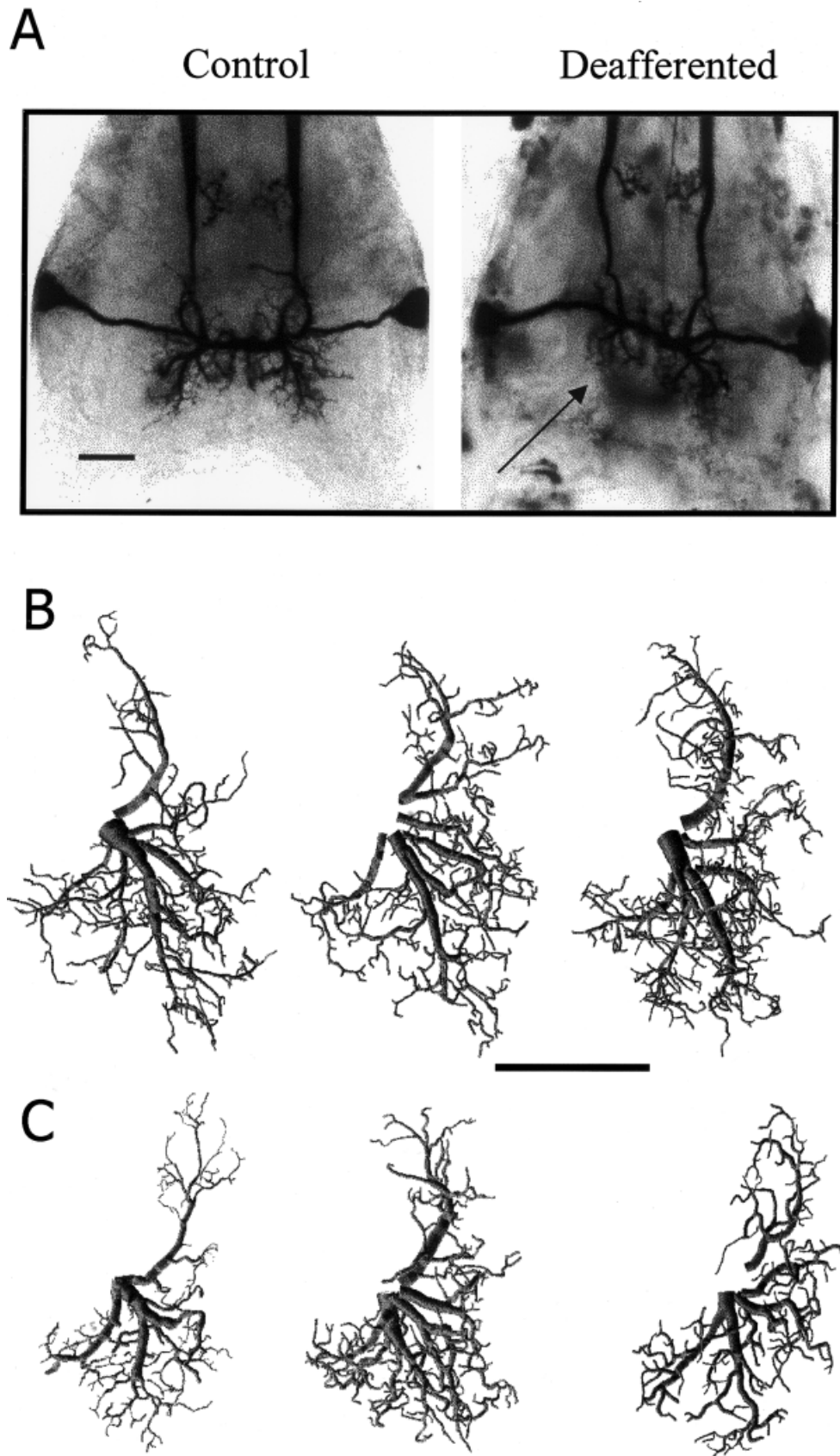


Fig. 2. The architecture of dendritic trees of deafferented GI2s. **A:** Photomicrographs of double staining of left and right GI2s from a control and a deafferented animal (left and right, respectively). Arrow points to the deafferented dendritic tree. **B:** Three examples of recon-

structed dendritic trees of control GI2s. **C:** Three examples of reconstructed dendritic trees of deafferented GI2s. Scale bars = 100 microns in A, 100 microns in B (applies to B,C).

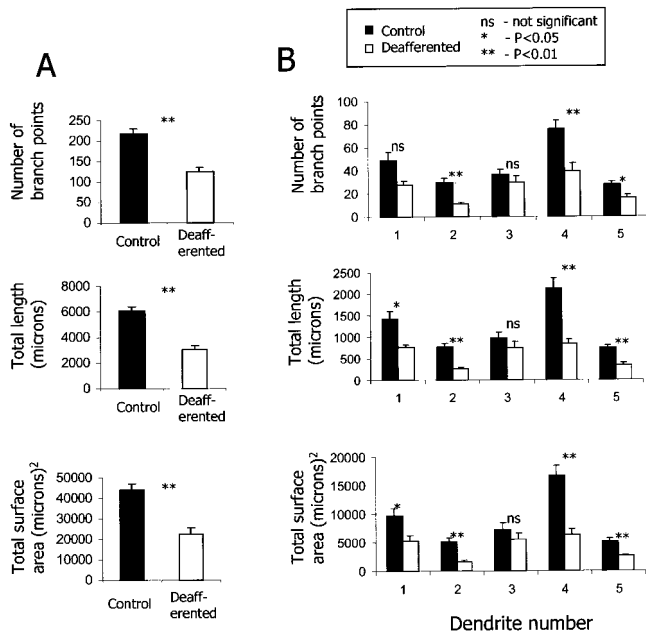


Fig. 3. Morphometric analysis of deafferented dendritic trees. **A:** Morphometric analysis of full dendritic trees. Histograms of the number of branch points, total length, and total surface area of the dendritic tree of GI2s from control (full bars) and deafferented (empty bars) animals. **B:** Morphometric analysis of each of the five identified dendritic trees of GI2. Histograms of the number of branch points, total length, and total surface area of the five identified dendritic trees of GI2 from control (full bars) and deafferented (empty bars) animals. Values represent average \pm SEM. Control, $n = 10$; deafferented, $n = 5$. Significant differences are indicated above the bars (t test; $*P < 0.05$, $**P < 0.01$).

deafferentation. For this, we first aligned the trees at the center and analyzed their gross spatial distribution by using Sholl analysis (Sholl, 1953). Two representative examples of dendritic trees from control (brown neuron) and deafferented (purple neuron) are shown separately (Fig. 4A) and in their aligned position within a schematic Sholl grid (Fig. 4B). The maximum distance occupied by the trees significantly decreased from 164 ± 6 to 116 ± 7 microns (Fig. 4C; t test, $P < 0.001$). The maximum number of branches was concentrated at a radius of 70 microns in the control animals and shifted to a radius of 50 microns in the deafferented animals. This was accompanied by a decrease in the maximum number of branch points from

56 ± 4 at 70 microns in the controls to 40 ± 4 at 50 microns in the deafferented animals. Thus, it seems that the most distal branches from the dendritic root either did not form or were pruned in the deafferented dendritic trees. However, Sholl analysis has been criticized for not discriminating between topologic and metrical aspects of

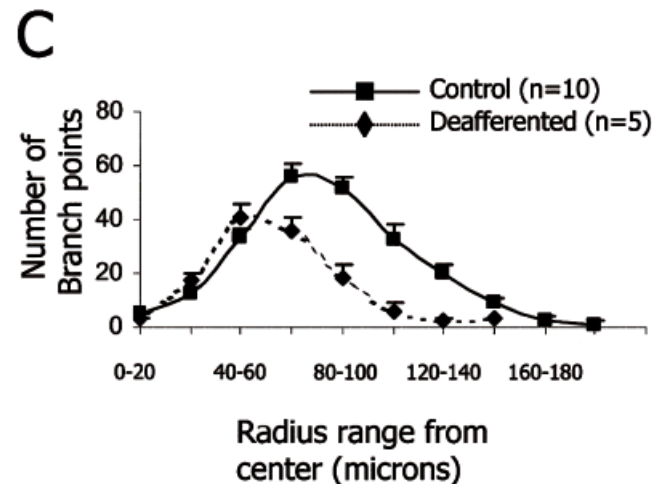
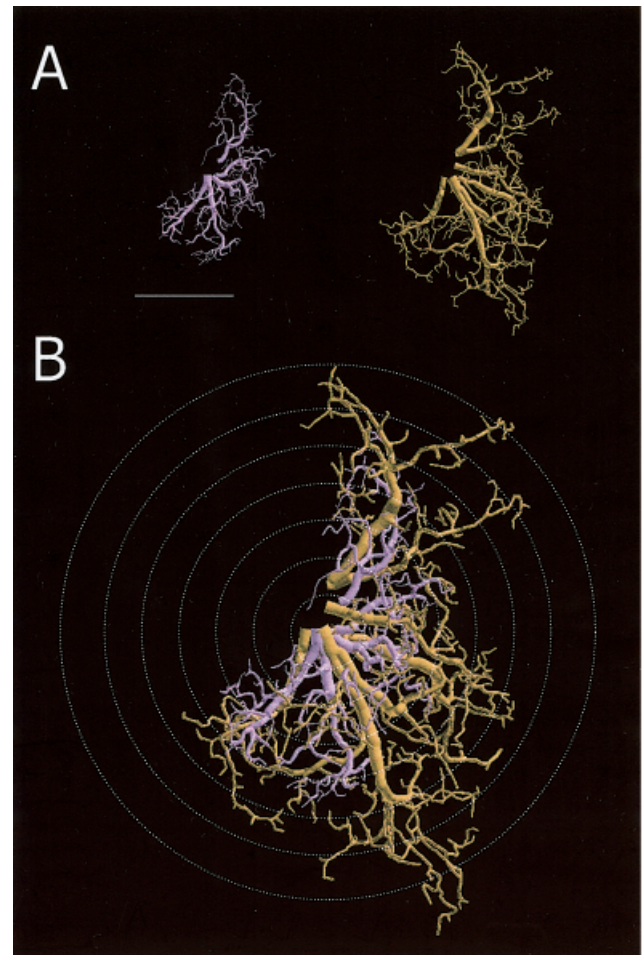


Fig. 4. Sholl analysis for control and deafferented dendritic trees. **A:** One reconstructed dendritic tree from a control animal (brown) and one from a deafferented animal (purple) shown separately. **B:** The two dendritic trees from A represented aligned to their axonal-dendritic junction. In Sholl analysis, the number of branch points is counted within each Sholl sphere (white dashed lines). **C:** Sholl plot showing the number of branch points (mean \pm SE) along the spheres from the center to the periphery. In control dendritic trees (solid line), the peak number of branch points is located at roughly 70 microns and the distribution of branch points ranges from 0 to 170 microns from the center. In deafferented dendritic trees (dashed line), the peak number of branch points is located at roughly 50 microns and the distribution of branch points ranges from 0 to 130 microns from the center. Scale bar = 100 microns in A.

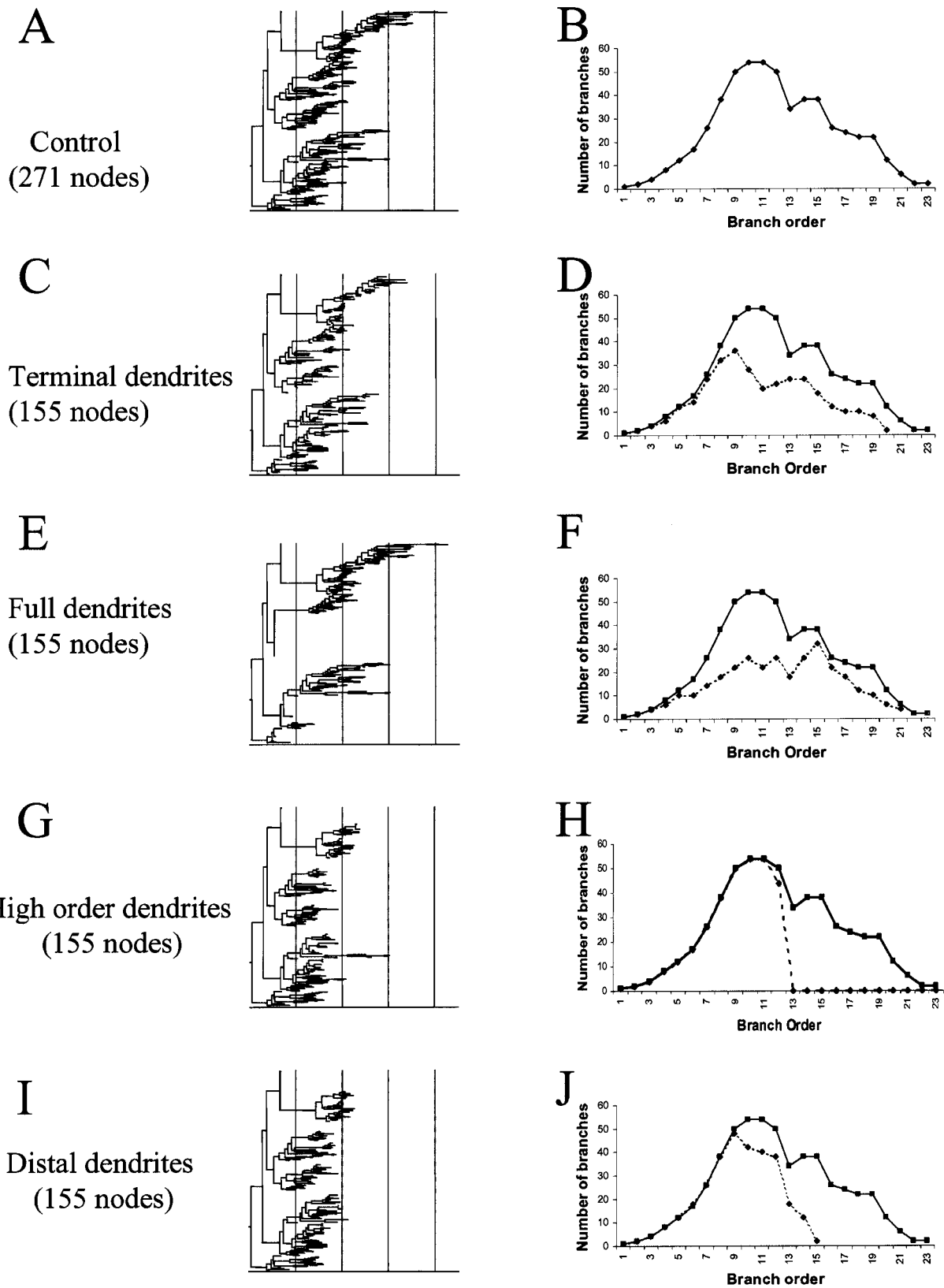


Fig. 5. Four models for dendritic pruning. **A:** A dendrogram from a control GI2 with 271 nodes. **B:** Branch order distribution of the dendrogram shown in A. **C–J:** Dendrograms and branch order distributions after pruning 116 nodes from the control dendritic tree in A. **C:** Terminal dendrites model. A dendrogram of the control dendritic tree after it has been pruned at terminal branches regardless of the branch order hierarchy. **D:** Branch order distribution of the dendrogram in D (dashed line) vs. control (solid line). **E:** Full dendrites model. A dendrogram of the control dendritic tree after it has been

pruned at distinct dendrites from tip to the root. **F:** Branch order distribution of the dendrogram in E (dashed line) vs. control (solid line). **G:** High-order dendrites model. A dendrogram of the control dendritic tree after it has been pruned at high-order branches. **H:** Branch order distribution of the dendrogram in G (dashed line) vs. control (solid line). **I:** Distal dendrites model. A dendrogram of the control dendritic tree after it has been pruned at distal branches. **J:** Branch order distribution of the dendrogram in I (dashed line) vs. control (solid line). Dendrogram scale = 100 microns.

tree structure (Uylings et al., 1986). Therefore, we constructed dendrograms and further analyzed these trees by using segment analysis, which is based on branch order. This analysis allows us to address separately some of the topologic aspects of these trees.

The number of branches in a tree may decrease according to several different models. Figure 5 shows four different possible ways of pruning branches from a control neuron. The corresponding branch order distribution is shown as a graph next to each dendrogram. Thus, Figure 5A and Figure 5B show a dendrogram of a control GI2 from our database and its branch order distribution, respectively. The dendritic tree from Figure 5A has 271 nodes distributed in 23 orders. Four different ways to prune this tree to 155 nodes (a constraint imposed by the morphometric analysis in Fig. 3) are shown in Figure 5C–J. In the first possibility, called terminal dendrites, the control dendritic tree is pruned only at random terminal branches regardless of their branch order (Fig. 5C). Because terminal branches from all orders are pruned, both the peak of the curve and the maximum number of branches will decrease, but the maximum branch order will be only mildly affected (Fig. 5D). In the second possibility called, full dendrites, full dendritic trees (from the tip to the root) are pruned (Fig. 5E). In this case, the maximum number of branches at the peak of the curve will decrease, whereas the maximum branch order will be only mildly affected (Fig. 5F). In the third possibility, called high-order dendrites, high-order branches are pruned (Fig. 5G). This pruning mildly affects the peak of the curve but results in sharp decrease of the maximum branch order (Fig. 5H). Finally, in the fourth possibility, called distal dendrites, most distal branches are pruned from the tree (Fig. 5I). Although this model of pruning resembles the high-order dendrites pruning model, the former is based on spatial distance regardless of branch order. This method of pruning will mildly affect the peak of the curve but will result in a substantial decrease in the maximum branch order (Fig. 5J).

The plots of branch order distribution for the control and the deafferented groups are shown in Figure 6A and appear to fit the distal dendrites model. For the lower branch order range (2–8), the frequency of branches is not significantly different between both groups. In addition, the two curves peak at similar branch orders (control, 9th order; deafferented, 8th order). Furthermore, the maximum number of branches is decreased from 40 ± 1 to 34 ± 5 but is not significantly different between the control and the deafferented groups (Fig. 6A; *t* test; $P > 0.05$). However, the maximum branch order is significantly decreased from 21 ± 0.9 orders in the controls to 16 ± 1.2 orders in the deafferented dendritic trees (Fig. 6A; *t* test; $P < 0.01$). Therefore, the branch order analysis strongly supports the Sholl analysis. Taken together, the Sholl and the branch order analyses suggest that sensory deprivation affects mainly the formation or the maintenance of distal high-order dendritic branches of the dendritic tree of GI2.

Deafferentation affects neither elongation nor branching

Dendritic development is eventually a process of elongation and branching (Cline, 2001). Branching of the low-order branches seems to be normal in deafferented animals because the number of branch points is remarkably

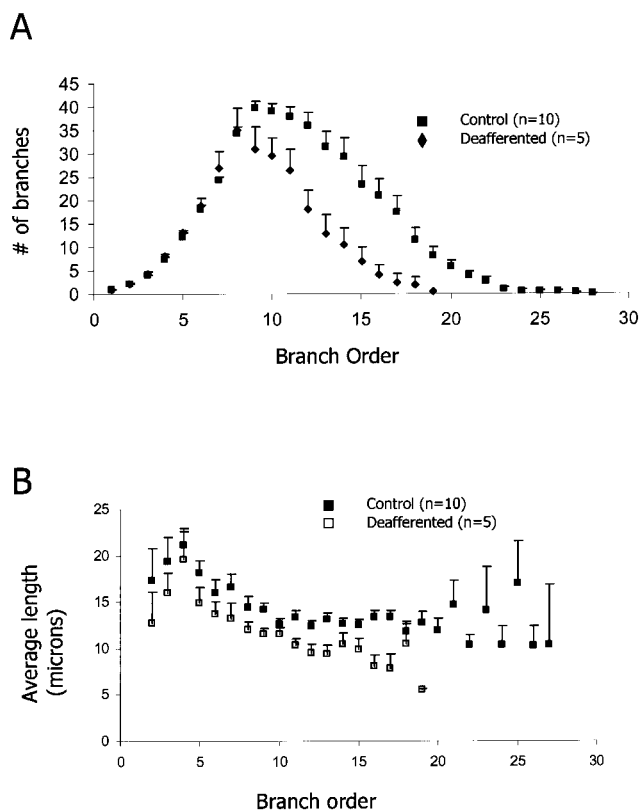


Fig. 6. Deafferentation affects high-order branching but not elongation of low-order branches. **A:** Distribution of the number of branches of the dendritic trees from control GI2s (squares) and the dendritic trees from deafferented GI2s (diamonds) as a function of branch order. The maximum number of branches is not significantly different between the groups (*t* test; $P > 0.05$). The maximum branch order is significantly lower in deafferented dendritic trees (*t* test; $P < 0.01$). **B:** Plot of dendritic segments length as a function of branch order for the control group (squares) and the deafferented group (open squares). For the comparable part of the graph (orders 2–19), the curves are not significantly different (analysis of variance; $P > 0.05$).

similar to the controls for the initial branch orders (see left part of the curve in Fig. 6A). To study whether elongation is affected, we compared the segment length of the control and deafferented dendritic trees. Figure 6B shows the segment length distribution at different branch orders for the control (squares) and the deafferented (open squares) dendritic trees. A comparison between the two groups across the same branch order range (orders 2–19), revealed no significant differences (ANOVA, $P > 0.05$). These results show that the deafferented dendritic trees developed normally at lower branch orders and suggests that, in this region of the tree, the innate capacity of the GIs to elongate and branch is not affected by afferent input.

Finally, we analyzed the topologic structure of the control and deafferented trees by calculating the tree asymmetry of the whole trees. Tree asymmetry values of the control dendritic trees (0.56 ± 0.04) were not significantly different from the values of the deafferented dendritic trees (0.52 ± 0.04) (*t* test; $P > 0.05$).

DISCUSSION

In this work, we explored the effects of sensory input deprivation on the dendritic geometry of an identified neuron. Our results indicate that the axonal terminals of sensory afferent neurons mostly affect development of high-order distal dendritic segments, with little effect on the lower order proximal dendritic segments. This result suggests that interactions between pre- and postsynaptic neurons play a specific regulatory role in the formation or maintenance of high-order distal dendritic branches of the GIs' trees.

Role of afferent innervation on dendritic formation

At the single cell level, a detailed quantitative analysis of the effects of afferent input on dendritic tree maturation has been performed on neurons characterized by a relatively simple dendritic geometry. One example is the identified Mauthner neurons of developing amphibians whose dendritic tree branch only two to three orders. In the Mauthner cell, deafferentation reduces, whereas supra-innervation enhances dendritic growth specifically in the deprived region (Goodman and Model, 1988). In addition, incoming axons stimulate dendritic growth in an activity independent manner (Goodman and Model, 1990). Another example is the early dendritic development of hippocampal neurons. Dendritic branch formation is induced by afferent innervation *in vitro* by means of both activity-dependent and activity-independent mechanisms (Kossel et al., 1997). Like for the Mauthner neuron, the effect is region specific because the effect of the afferents is observed only on dendrites, which established contact with the afferents. In that respect (in the case of GI2), it is possible that cercal afferents in GI2 do not establish synapses with this region of the tree because identified dendrite number 3 did not change after deafferentation. Jacobs and Theunissen (2000) recently have shown spatial segregation of input on the dendritic tree of a GI whereby different regions of the tree receive inputs from different sets of cercal afferents. Our results support the idea that there is such a functional partition of afferent input on the dendritic arbor of GI2.

In crickets, sensory deprivation induces dendritic growth of the medial dendrites and a concomitant decrease of the lateral dendrites of an auditory interneuron (Hoy et al., 1985). GI2, like most GIs, has small contralateral dendrites branches that sprout from the link segment in the contralateral portion of the neuropile (Daley et al., 1981). These short and mostly unbranched dendrites receive subthreshold afferent input from a few columns of hairs located on the contralateral cercus (Daley and Camhi, 1988). When the ipsilateral cercus is ablated, the input from the contralateral cercus is enhanced (Volman and Camhi, 1988; Volman, 1989). To examine whether the morphology of these contralateral dendrites is affected by amputation of the ipsilateral cercus, we reconstructed these small dendrites in a few deafferented and control GI2s. Morphometric analysis shows no obvious differences between the two groups of cells. The number of contralateral dendrites per neuron, total length, total surface area, and total volume were not significantly different between the control and experimental groups (data not shown). This finding suggests that the change in the efficacy of the

contralateral input after long-term deafferentation is not correlated with structural changes of the postsynaptic dendritic targets.

Analysis of dendritic branching

Given that metrics and topology are different aspects of tree structure they must be analyzed separately (Uyulings et al., 1986). The interpretation of Sholl analysis is limited, because this analysis does not discriminate between these two aspects of tree structure. In the present study, we examine separately both the metric and the topologic properties of the dendritic trees of GIs. The branch order analysis complements the results of the Sholl analysis in that it suggests that changes are indeed confined to the distal branches of the deafferented tree rather than lower order branches. The deafferented dendritic tree is neither a shrunken version of the adult neuron nor does it seem to be topologically reorganized as depicted by the similar tree asymmetries.

Morphologically, dendritic trees expand by both elongation of the dendritic segments and branching. Neuronal branching can occur by formation of new branches at the terminals and/or by preterminal branching (Acebes and Ferrus, 2000). Are either of these growth mechanisms affected by the absence of afferent input? Although modern imaging techniques have been used to identify modes of growth (Dailey and Smith, 1996; Wu et al., 1999), these techniques are difficult to implement on a long time scale. In our work, we can only speculate as to whether deafferentation affects elongation, bifurcation, or interstitial branching. However, our quantitative analyses indicate a high degree of structural similarity between controls and the deafferented trees at lower branch orders. Thus, it seems that neither elongation nor branching is significantly affected at lower branch orders. Rather, the effect of deafferentation is confined to a specific periphery of the dendritic arbor without affecting the intrinsic mechanisms of formation of the core of the dendritic arbor.

Role of synaptic activity on the development of dendrites

Axonal navigation and appropriate synaptic connection can be precisely achieved at initial stages of development in an activity-independent manner. Knockout mice completely lacking neurotransmitter secretion develop normal layered structures, normal fiber pathways, and morphologically defined synapses (Verhage et al., 2000). Thus, the initial assembly of neuronal circuitry seems activity independent, whereas neuronal (and synaptic) maintenance appears to be activity dependent. For instance, synaptic input is closely linked to structural stability of dendrites in the somatosensory barrel cortex (Wallace and Fox, 1999; Lendvai et al., 2000). Thus, as a general rule, synaptic activity is critical at later stages of development where it refines and stabilizes existing connections (for review see also Goodman and Shatz, 1993; Katz and Shatz, 1996; Tessier-Lavigne and Goodman, 1996). It seems that the cockroach central nervous system obeys a similar rule of wiring, as functional synapses between the sensory axons and the GIs form before the onset of afferent activity (Blagburn et al., 1996). In addition, synaptic activity has been shown to be important in the enhancement of the excitability of deafferented GIs but had little effect on the excitability in the nondeafferented GIs (Vol-

man and Camhi, 1988). This finding suggests that the absence of synaptic activity has little consequence on the fine dendritic architecture of the GIs, whereas deafferentation does.

Role of environmental factors in the development of dendrites

In addition, a dimensional constraint may be induced by the change in the volume of the neuropile. Estimation of the volumetric change of the neuropile of deafferented cercal system of crickets has shown a correlation between the scaling down of the neuropile and the shortening of the dendrites (Murphey et al., 1975). However, the possibility of a causal link between changes in the dimensions of the neuropile and dendritic trees is unlikely for the following two reasons. First, we have found no correlations between the size of the ganglion and the size of dendritic trees of specific GIs (Mizrahi et al., 2000). Second, the present study shows that different dendrites of GI2 are selectively affected to a different extent one of which appears to develop to full size (Fig. 3B). Given these results, the decrease in dendritic size is unlikely to be due to shrinkage of the neuropile.

To conclude, dendritic tree maturation of the GIs is regulated by extrinsic (environmental) as well as intrinsic (genetic) factors. In the cercal system, intrinsic factors might govern the basic (lower order) branching pattern of the dendritic tree, whereas extrinsic factors might play an important role in the formation or maintenance of the distal higher order branches. In addition, the ability of neurons to branch and elongate appears to be, at least, to some extent, innate because it is not affected by deafferentation.

ACKNOWLEDGMENTS

We thank J. Schaeffer and A. Weisel-Eichler for critically reading and improving the manuscript. These experiments comply with Principles of Animal Care, NIH publication no. 86-23, revised in 1985, and also with the current laws of the State of Israel.

LITERATURE CITED

- Acebes A, Ferrus A. 2000. Cellular and molecular features of axon collaterals and dendrites. *TINS* 23:557–565.
- Blagburn JM, Beadle DJ. 1982. Morphology of identified cercal afferents and giant interneurons in the hatchling cockroach *Periplaneta americana*. *J Exp Biol* 97:421–426.
- Blagburn JM, Beadle DJ. 1984. Synapses between an identified giant interneuron and a filiform hair sensory neuron in the terminal ganglion of first instar cockroaches *Periplaneta americana*. *J Exp Biol* 113:477–481.
- Blagburn JM, Thompson KSJ. 1990. Specificity of filiform hair afferent synapses onto giant interneurons in *Periplaneta americana*: anatomy is not a sufficient determinant. *J Comp Neurol* 302:255–271.
- Blagburn JM, Sosa MA, Blanco RE. 1996. Specificity of identified central synapses in the embryonic cockroach: appropriate connections form before the onset of spontaneous afferent activity. *J Comp Neurol* 373:511–528.
- Bugnion E. 1921. The growth of the antenna and cerci of the cockroach, *Periplaneta americana*. *Bull Entomol Soc Egypt Econ Ser* 6:56–66.
- Camhi JM. 1984. Neuroethology. Sunderland: Sinaur Association.
- Chiba A, Shepherd D, Murphey RK. 1988. Synaptic rearrangement during postembryonic development in the cricket. *Science* 240:901–905.
- Cline HT. 1999. Development of dendrites. In: Stuart G, Spruston N, Häusser M, editors. *Dendrites*. New York: Oxford University Press. p 35–67.
- Cline HT. 2001. Dendritic arbor development and synaptogenesis. *Curr Opin Neurobiol* 11:118–126.
- Dagan D, Volman S. 1982. Sensory basis for directional wind detection in first instar cockroaches, *Periplaneta americana*. *J Comp Physiol* 147:471–478.
- Dailey ME, Smith SJ. 1996. The dynamics of dendritic structure in developing hippocampal slices. *J Neurosci* 16:2983–2994.
- Daley DL, Camhi JM. 1988. Connectivity pattern of the cercal-to-giant interneuron system of the American cockroach. *J Neurophysiol* 60:1350–1367.
- Daley DL, Vardi N, Appignani B, Camhi JM. 1981. Morphology of the giant interneurons and cercal nerve projections of the American cockroach. *J Comp Neurol* 196:41–52.
- Deitch JS, Rubel EW. 1984. Afferent influences on brain stem auditory nuclei of the chicken: time course and specificity of dendritic atrophy following deafferentation. *J Comp Neurol* 229:66–79.
- Goodman LA, Model PG. 1988. Superinnervation enhances the dendritic branching pattern of the Mauthner cell in the developing axolotl. *J Neurosci* 8:776–791.
- Goodman LA, Model PG. 1990. Eliminating afferent impulse activity does not alter the dendritic branching of the amphibian Mauthner cell. *J Neurobiol* 21:283–294.
- Goodman CS, Shatz CJ. 1993. Developmental mechanisms that generate precise patterns of neuronal connectivity. *Cell* 72(Suppl):77–98.
- Gray L, Smith Z, Rubel EW. 1982. Developmental and experimental changes in dendritic symmetry in n. laminaris of the chick. *Brain Res* 244:360–364.
- Hamon A, Guillet JC, Callec JJ. 1994. Patterns of monosynaptic input to the giant interneurons 1–3 in the cercal system of the adult cockroach. *J Comp Physiol* 174:91–102.
- Hill AAV, Edwards DH, Murphey RK. 1994. The effect of neuronal growth on synaptic integration. *J Comput Neurosci* 1:239–254.
- Hoy RR, Nolen TG, Casaday GC. 1985. Dendritic sprouting and compensatory synaptogenesis in an identified interneuron follow auditory deprivation in a cricket. *Proc Natl Acad Sci U S A* 82:7772–7776.
- Jacobs GA, Nevin R. 1991. Anatomical relationships between sensory afferent arborizations in the cricket cercal system. *Anat Rec* 231:563–572.
- Jacobs GA, Theunissen FE. 2000. Extraction of sensory parameters from a neural map by primary sensory interneurons. *J Neurosci* 20:2934–2943.
- Katz LC, Shatz CJ. 1996. Synaptic activity and the construction of cortical circuits. *Science* 274:1133–1138.
- Koch C, Segev I. 2000. The role of single neurons in information processing. *Nat Neurosci* 3:1171–1177.
- Kossel AH, Williams CV, Schweizer M, Kater SB. 1997. Afferent innervation influences the development of dendritic branches and spines via both activity-dependent and non-activity-dependent mechanisms. *J Neurosci* 17:6314–6324.
- Lendvai B, Stern EA, Chen B, Svoboda K. 2000. Experience-dependent plasticity of dendritic spines in the developing rat barrel cortex in vivo. *Nature* 404:876–881.
- Mainen ZF, Sejnowski TJ. 1996. Influence of dendritic structure on firing pattern in model neocortical neurons. *Nature* 382:363–366.
- Mizrahi A, Ben-Ner E, Katz MJ, Kedem K, Glusman JG, Libersat F. 2000. Comparative analysis of dendritic architecture of identified neurons using the Hausdorff distance metric. *J Comp Neurol* 422:3 415–428.
- Murphey RK, Mendenhall B, Palka J, Edwards JS. 1975. Deafferentation slows the growth of specific dendrites of identified giant interneurons. *J Comp Neurol* 159:407–418.
- Rall W, Burke RE, Holmes WR, Jack JJ, Redman SJ, Segev I. 1992. Matching dendritic neuron models to experimental data. *Physiol Rev* 72:S159–S186.
- Ritzmann RE. 1984. The neural organization of cockroach escape and its role in context dependent orientation. In: Beer RD, Ritzmann RE, McKenna T, editors. *Biological neural networks in invertebrate neuroethology and robotics*. New York: Academic Press. p 113–137.
- Scott EK, Luo L. 2001. How do dendrites take their shapes? *Nat Neurosci* 4:359–365.
- Sholl DA. 1953. Dendritic organization in the neurons of the visual cortex and motor cortices of the cat. *J Anat* 87:387–406.

- Smith ZD, Gray L, Rubel EW. 1983. Afferent influences on brainstem auditory nuclei of the chicken: n. laminaris dendritic length following monaural conductive hearing loss. *J Comp Neurol* 220:199–205.
- Tessier-Lavigne M, Goodman CS. 1996. The molecular biology of axon guidance. *Science* 274:1123–1133.
- Uylings HB, Ruiz Marcos A, van Pelt J. 1986. The metric analysis of three-dimensional dendritic tree patterns: a methodological review. *J Neurosci Methods* 18:127–151.
- van Pelt J, Uylings HB, Verwer RW, Pentney RJ, Woldenberg MJ. 1992. Tree asymmetry: a sensitive and practical measure for binary topological trees. *Bull Math Biol* 54:759–784.
- Verhage M, Maia AS, Plomp JJ, Brussaard AB, Heeroma JH, Vermeer H, Toonen RF, Hammer RE, van den Berg TK, Missler M, Geuze HJ, Sudhof TC. 2000. Synaptic assembly of the brain in the absence of neurotransmitter secretion. *Science* 287:864–869.
- Vetter P, Roth A, Hausser M. 2001. Propagation of action potential in dendrites depends on dendritic morphology. *J Neurophysiol* 85:926–937.
- Volman SF. 1989. Localization of the enhanced input to cockroach giant interneurons after partial deafferentation. *J Neurobiol* 20:762–783.
- Volman SF, Camhi JM. 1988. The role of afferent activity in behavioral and neuronal plasticity in an insect. *J Comp Physiol* 162:781–791.
- Wallace H, Fox K. 1999. Local cortical interactions determine the form of cortical plasticity. *J Neurobiol* 41:58–63.
- Wu GY, Zou DJ, Rajan I, Cline H. 1999. Dendritic dynamics in vivo change during neuronal maturation. *J Neurosci* 19:4472–83.